

Dear Dr. Gerasopoulos,

Please find attached the response to the reviewer comments. Moreover, I highlighted in red font color the main changes in the revised text. I did not include very obvious and small changes, typos and so on, in this “red version”, but they are done as mentioned in the responses.

Kind regards,

Antti Arola

We would like to first express our thanks to the **REFEREE #1** for his/her constructive comments. The responses to these are below after the reviewer points that are in bold.

The manuscript “Measurement-based direct radiative effect by brown carbon over Indo-Gangetic Plain” by Arola et al. presents a novel approach to determining the total aerosol, black carbon (BC), and brown carbon (BrC) direct radiative effect (DRE) using AERONET inversion data products obtained from four AERONET sites in the Indo-Gangetic Plain region. In addition to providing valuable information regarding the sign and magnitude of the DREs, the manuscript details a unique analysis on the seasonality of the DRE for each aerosol type. Overall, the manuscript presents interesting results to a solid analysis and would make a nice contribution to ACP. However, before publication, I believe the following points should be addressed:

-Some statistics on the relevant parameters are needed. Error bars representing one standard deviation on the monthly averages should be included on all the panels in Fig. 3. How variability in these parameters impact monthly differences in the DREs should be assessed in order to confirm the seasonal cycle.

In the revised version, we included a new box-plot figure (thus including also the variability, through 25% and 75% percentiles, in addition to median and mean) of monthly imaginary indices at RNIR wavelengths and the difference between 440nm and RNIR. The former essentially determines our BC and the latter BrC concentrations. This had to be a separate and new plot, since the Figure 3 would not have remained clear and readable enough with several error bars. The variability in these imaginary indices contains the major information regarding also the amount of variability in our retrieved fractions of absorbing components and thus in our DRE calculations. For this reason, we presented only the variability in the parameters of the upper panels of Figure 3 (in the previous version), as the clear link between the upper and other panels is stressed.

We did not, however, conduct new simulations to assess whether the variability in BC and BrC fractions could affect the seasonal cycle that we have obtained. If the DRE calculations were made fully consistently, this would have required to start from the actual retrievals of BC and BrC fractions, with assumed variability in the input information (imaginary indices). Alternatively, we made a rough assessment by looking at the variability of BC and BrC fractions at the months of largest warming and cooling (in the Figure 3 of the revised version). This figure confirms that there is essentially no overlap in BC fractions between these months and thus suggests that the variability overall (BC and BrC) is not nevertheless large enough to substantially mask our clear seasonality of BrC DRE. This is briefly stressed in the revised version.

-As suggested by Lack and Cappa (2010) and Kim et al. (2015) there may be a spectral dependence of kBC, especially those particles containing coatings. Some analysis or discussion on how a spectrally-dependent kBC would impact the calculated BrC volume fractions (and thus the BrC DREs) should be included in the text. Alternatively, if the assumption that considering only pure, uncoated BC is indeed valid for this region and/or this method, this should be stated and supported with references.

Lack and Cappa 2010 did not discuss spectral variability of kBC at all. And in Kim et al. 2015 (if we

now talk about the same paper), the dependence was very minor indeed: from 0.67 at 467nm to 0.63 at 660nm. We are assuming a mixing scenario that is similar to Lack and Cappa, that is internal mixing; however, we are assuming a homogeneous internal mixture, whereas Lack and Cappa assumed a BC core with a BrC coating. We are using a homogeneous internal mixture, because that is what is used in the AERONET retrieval.

-It is my understanding the BrC refractive index (and its spectral dependence) are not well established. A reference and reason as to why the selected BrC refractive index was used would be helpful, even if this is already stated in the referenced Schuster et al. (2015a) paper.

It is certainly true that there exists a wide range of published values of k_{BrC} . We use Kirchstetter et al. 2004 for our baseline refractive index of BrC, because it provides reasonable maximum and median fractions for BrC and also reasonable BrC/BC ratios. This has been discussed in Schuster et al. 2015a and is now also briefly mentioned, as a justification, in our revised version.

-The results section (Section 3, starting on page 21591, line 5) was a bit confusing; as is, the discussion jumps back and forth between Fig. 4 and 5 too much. I suggest restructuring it so that the discussion and description of the more generalized relationship between BrC and BC volume fractions and the differences in k (i.e., Fig. 5) precedes the discussion of the time series in Fig. 4. Also the lines in the bottom panel of Fig. 5 are confusing. I understand each point represents the monthly average BC and BrC volume fractions starting with January at the star but it's not clear it's really showing anything valuable. I recommend only plotting April and November (the middle of the two interesting periods) or removing them all together and referring to Fig. 3.

Thanks for pointing out the need for clarified discussion between these two Figures (Figure 5 and 6 of the revised version). First, however, we want to emphasize the definite need to keep the Figure 5, which brings information that cannot be conveyed from the Figure 3. However, we modified the figure and hopefully it is now easier to interpret. It includes now only two months, as suggested by the reviewer. Moreover, we excluded a separate upper panel of 440nm case and included the difference in imaginary index at 440nm as isolines in the lower RNIR plot. Therefore, the current figure includes only one panel and contains much more information in a one glance. In addition, we tried to make the link between these two figures (Figures 4 and 5) more obvious to the reader.

-Two of the most interesting and important findings of this work are 1) the seasonality in BrC radiative forcing and 2) the fact assuming spectrally-invariant BrC can result in offsets upwards near a factor of 2 in BrC DRE. However, the significance of these results seems to get a bit lost in the comparison to the total aerosol DRE which appears to have no relationship seasonally or otherwise to BrC DRE. Further, because this comparison occurs at the very end of the discussion, it leaves the reader with a bit of "so what?" feeling. I suggest re-framing the big picture and focusing more on the potential errors introduced in the estimated positive forcing associated with carbonaceous aerosols when BrC DRE is neglected. This can be done by including a panel showing the monthly contribution of BrC DRE to total carbonaceous aerosol DRE (BrC +BC) as a ratio or percentage, either in addition to or in replacement of the BC DRE in Fig. 6 and adding some corresponding text in the discussion. This would show that, while BrC

might be a minor contributor to the total aerosol effect in this region, it does contribute with some significance to uncertainties in the positive RF (upwards near 10% for some months based on Fig. 6) associated with aerosol absorption.

In the revised version, we slightly modified the “big picture” as suggested with more discussion regarding the BrC impact in total carbonaceous effect as well. Overall we included results of different DREs (Total, BC, BrC) in a Table 3 of the revised version, which is useful to estimate quantitative importance of BrC from different point of view.

Other specific comments:

Title: I’m not sure if this should be considered “measurement-based” since the analysis relies on parameters obtained indirectly (retrieved) from radiance and direct-sun measurements. I would suggest removing “measurement-based” and starting the title either as “Retrieved direct-radiative: : :” or just “Direct-radiative: : :”

The title has been modified.

Page 21586, line 25 and Page 21587, lines 7-8: So are Level 1.5 or Level 2.0 size distributions used? Clarify.

Yes, we agree that these statements became confusing. For size distributions we ended up using only Level 2 data. This has been now clarified.

Page 21589, lines 3-8: For those instances in which dust is placed in the fine mode, how is BrC distinguished from dust for k440? Do any of these instances occur in March-May? If yes, how does this impact the results shown for the pre-monsoon dust season (March-May) when BrC is noted to have a high BrC volume fraction?

Page 21589, lines 28-29: See above. If goethite and hematite were not distinguished from BrC in the fine mode, could the enhancement in BrC volume fraction be because it is really a BrC + fine-mode dust estimate?

This is to answer both two comments above. The algorithm of Schuster et al. 2015a places dust in the fine mode, when AERONET indicates a very strong spectral dependence of the imaginary index (as indicated by the branch A of their Figure 6). In these cases, it is assumed that there is zero BrC in the fine mode, so there is no risk of overestimating the contribution of BrC to the fine mode in these cases, while underestimation is possible. However, these cases did not occur in our results, i.e. we did not have dust in fine mode in any month. An opposite problem could then happen though: in reality, there should have been fine mode dust, while the algorithm placed only BrC to account for the spectral dependence of imaginary index. These cases, of course, would impact our estimations. However, there is no way to estimate the probability of these cases, when the evidence generally about the dust in fine mode is missing as well.

Page 21593, lines 20-25: What are the values compared to the non-BrC DREs? A table of these values would be useful.

There is a new table hopefully giving enough interesting details regarding the DRE of BrC in relation to the radiative effect of other components.

Minor editorial comments:

Page 21584, line 4: Remove “those” in second sentence.

Done.

Page 21585, line 1: Need an “and” before (2).

Done.

Page 21586, line 7: AERONET does both a direct-sun and sky radiance measurements at 440, 670, 870, and 1020nm. Add “also” between “are” and “used” to make this clearer.

Done.

Page 21592, line 24: Remove “best.”

Done.

Page 21594, line 8: Add “an” between “using” and “identical.”

Done.

We would like to first express our thanks to the **REFEREE #2** for his/her constructive comments. The responses to these are below after the reviewer points that are in bold.

General Comments: This is a well-written and informative paper regarding aerosol Brown Carbon (absorbing Organic Carbon) and computed aerosol forcing effects in a very important aerosol source region (the IGP region of India and Pakistan). I believe this paper clearly meets the standards of ACP and makes a useful contribution to the literature, and should be published with only suggested minor revisions (see below).

Specific Comments:

Page 21586, lines 5-6: The AERONET UV filters (340 and 380 nm) have a full width at half maximum (FWHM) of 2 nm as compared to 10 nm for all other channels.

This is now corrected.

Page 21586, line 17: The AOD is larger than 0.5 at 440 nm (include the wavelength)

Wavelength is now included.

Page 21587, lines 18-19: The IGP is bounded to the north by the Himalayan foothills and to the south by lower altitude mountains.

Sentence modified as suggested.

Page 21587, lines 25-27: It would be useful to know if these monthly mean AOD values in Figure 2 are computed from the all of the Level 2 direct sun measurements (most robust method to compute mean climatology of AOD) or from only those direct sun measurements associated with almucantar retrievals.

In our case, mean AODs were based on almucantar retrievals only (thus taken from inversion product, not from direct sun, which would have been more appropriate). This is now clarified.

Page 21587, lines 27-29: Perhaps you could provide the percentage of total retrievals that were L2 retrievals of the entire data set utilized in this study.

These percentages are now included in the text.

Page 21589, lines 8-9: Please clarify, are the number of imaginary indices the number of almucantar retrievals?

This is correct and is now clarified in the text.

Page 21589, line 15: Is the total volume mentioned here for the fine mode only or both

fine and coarse modes?

It was for both fine and coarse mode. This has been now clarified.

Page 21591, lines 1-2: Please briefly describe how you extended the four wavelengths of the albedo data from AERONET retrieval input data (440, 675, 870 and 1020 nm) to the total SW spectrum.

This has been now explained in the revised version.

Page 21595, lines 6-8: Maybe you could mention the advantage here of your approach in the ability to separate dust from BrC absorption.

Now this advantage is briefly mentioned.

Page 21595, Conclusions: You might consider mentioning how critical the BrC absorption is for UV radiation and remote sensing from satellite in the UV wavelengths (i.e. OMI, etc.). Alternatively this could be added to the Introduction if you feel it is not too disruptive of the flow of the paper.

This has been now briefly mentioned in the conclusions.

Direct radiative effect by brown carbon over Indo-Gangetic Plain

A. Arola¹, G.L. Schuster², M.R.A. Pitkänen^{1,3}, O. Dubovik⁴, H. Kokkola¹, A.V. Lindfors¹, T. Mielonen¹, T. Raatikainen⁵, S. Romakkaniemi¹, S.N. Tripathi^{6,7}, and H. Lihavainen⁵

¹Finnish Meteorological Institute, Kuopio, Finland.

²NASA Langley Research Center Hampton, VA, USA.

³Department of Applied Physics, University of Eastern Finland, Kuopio.

⁴LOA, Université de Lille1/CNRS, Villeneuve d'Ascq, France

⁵Finnish Meteorological Institute, Helsinki, Finland.

⁶Department of Civil Engineering, Indian Institute of Technology, Kanpur, India.

⁷Centre for Environmental Science and Engineering, Indian Institute of Technology, Kanpur, India.

Correspondence to: Antti Arola
(antti.arola@fmi.fi)

Abstract.

The importance of light absorbing organic aerosols, often called brown carbon (BrC), has become evident in recent years. However, there are relatively few measurement-based estimates for the direct radiative effect of BrC so far. In earlier studies, the AEROSOL ROBOTIC NETWORK (AERONET) measured Aerosol Absorption Optical Depth (AAOD) and Absorption Angstrom Exponent (AAE) have been exploited. However, these two pieces of information are clearly not sufficient to separate properly carbonaceous aerosols from dust, while imaginary indices of refraction would contain more and better justified information for this purpose. This is first time that the direct radiative effect (DRE) of BrC is estimated by exploiting the AERONET-retrieved imaginary indices. We estimated it for four sites in Indo-Gangetic Plain (IGP), Karachi, Lahore, Kanpur and Gandhi College. We found a distinct seasonality, which was generally similar among all the sites, but with slightly different strengths. The monthly warming effect up to 0.5 W/m^2 takes place during spring season. On the other hand, BrC results in overall cooling effect in the winter season, which can reach levels close to -1 W/m^2 . We then estimated similarly also DRE of black carbon and total aerosol, in order to assess the relative significance of BrC radiative effect in the radiative effects of other components. Even though BrC impact seems minor in this context, we demonstrated that it is not insignificant and moreover that it is crucial to perform spectrally resolved radiative transfer calculations to obtain good estimates for DRE of BrC.

1 Introduction

20 Aerosols affect the Earth’s climate both directly (by scattering and absorbing radiation) and indi-
rectly (by serving as nuclei for cloud droplets). Currently, aerosol forcing is the largest uncertainty
in assessing the anthropogenic climate change (Myhre, 2013). Specifically, the role of carbona-
ceous aerosols is poorly understood. These particles can be divided into two categories: (1) Black
25 carbon (BC) is the main absorbing component present in atmospheric aerosols; and (2) Organic car-
bon (OC) represents a significant and sometimes major (20–90%) mass fraction of the sub-micron
aerosol (Kanakidou et al., 2005; Zhang et al. , 2007). Organic carbon has been most often assumed,
in global models for instance, to be non or only slightly absorbing component. However, there is
a growing evidence that a substantial amount of organic aerosols absorb at UV and visible wave-
lengths, particularly strongly at shorter wavelengths (e.g., Kirchstetter et al., 2004; Martins et al.,
30 2009). Nevertheless, so far there are only relatively few measurement-based estimates for the direct
radiative effect (DRE) of absorbing organic carbon, often called brown carbon, BrC. Both Chung
et al. (2012) and Feng et al. (2013) exploited AEROSOL ROBOTIC NETWORK (AERONET) measure-
ments to derive the radiative effect by BrC; the former used an approach to separate dust and car-
bonaceous aerosols based on AERONET-measured Absorption Angstrom Exponent (AAE), while
35 the latter accounted for short-wave enhanced absorption by BrC in their global model and demon-
strated an improved correspondence of modeled Aerosol Absorption Optical Depth (AAOD) and
AERONET measurements, when BrC absorption was included in the model.

The approach of Chung et al. (2012) has evident difficulties in separating dust and carbonaceous
by using AAE, and arguably an approach using AERONET-retrieved imaginary indices of refrac-
40 tion would be more justified, as discussed also in Schuster et al. (2015a, b). We estimated the BrC
fractions by using the method of Schuster et al. (2015a) for four AERONET sites in Indo-Gangetic
Plain (IGP), Karachi, Lahore, Kanpur and Gandhi College, and then calculated the corresponding
radiative effect by BrC. We moreover calculated similarly the DRE of BC and total aerosol, in order
to assess the relative significance of BrC radiative effect in carbonaceous or total aerosol radiative
45 effects.

2 Data and Methods

2.1 AERONET data

AERONET (AEROSOL ROBOTIC NETWORK) is a globally distributed network of automatic sun and sky
scanning radiometers that measure at several wavelengths, typically centered at 0.34, 0.38, 0.44,
50 0.50, 0.67, 0.87, 0.94, and 1.02 μm . The AERONET UV filters (340 and 380 nm) have a full width
at half maximum (FWHM) of 2 nm as compared to 10 nm for all other channels. All of these
spectral bands are utilized in the direct Sun measurements, while four of them are also used for the

sky radiance measurements, 0.44, 0.67, 0.87 and 1.02 μm . Spectral aerosol optical depth (AOD) is obtained from direct sun measurements, and inversion products of other aerosol optical properties, such as single scattering albedo (SSA), refractive indices and the column integrated aerosol size distributions above the measurement site are provided at the sky radiance wavelengths (Holben et al., 1998).

The estimated uncertainty in AOD (Level 2) is 0.01-0.02 and is primarily due to the calibration uncertainty (Eck et al., 1999). The uncertainty in complex index of refraction depends on AOD; Dubovik et al. (2000) estimated errors on the order of 30%–50% for the imaginary part and 0.04 for the real part of the refractive index for the cases of high aerosol loading (AOD at 440nm larger than 0.5). Aerosol loading is very high in IGP region, therefore these uncertainty estimates are likely representative for our AERONET sites as well.

Since the shortest sky radiance wavelength is 440nm, AERONET wavelengths are not ideal to detect BrC absorption, which is much stronger at shorter than 440nm wavelengths. However, it is also stressed that AOD is very high for all sites that were analyzed, allowing for sufficient robustness in the retrieved spectral signal in the imaginary refractive index.

In our study, we used Level 2 data of size distributions and refractive indices at four retrieval wavelengths 0.44, 0.67, 0.87 and 1.02. Moreover, we also included some Level 1.5 refractive indices, when $0.2 < \text{AOD}(440) < 0.4$, but only when a quality-checked Level 2 size distribution exists. In other words, we applied otherwise the same rigorous quality control that is required for Level 2 data, but we only relaxed the AOD requirement at 440nm from 0.4 to 0.2. We selected on purpose also these cases of possibly somewhat lower AOD, in order to not bias our sample, and thus estimate of DRE, towards higher aerosol loading. However, AOD at 440nm is typically above 0.4 in IGP region, so the set of almucantar refractive indices that we included turned out to be insignificantly different to that of the “full” Level 2 (not shown).

We included four AERONET sites for our data analysis, covering wide conditions in the Indo-Gangetic Plain (IGP): Karachi and Lahore in Pakistan, and Kanpur and Gandhi College in India. The measurements covered the following time periods, Gandhi College: 4/2006-3/2010; Kanpur: 1/2001-4/2012; Karachi: 9/2006-8/2011, Lahore: 4/2007-10/2011. Figure 1 shows the locations of these sites overlaid in the annual mean AOD map from MODIS Terra. In the IGP there are large local emissions of aerosols from various sources: heavy particulate pollution from industrial sources, strong vehicular emissions, use of fossil fuels, and widespread biomass and agricultural crop residue burning. In addition, the IGP is strongly affected by seasonal (pre-monsoon) mineral dust transported mainly from the Thar desert (e.g., Jethva et al., 2005; Ram et al., 2010; Kedia et al., 2014). The seasonal monsoon rains are extremely vital for IGP and strongly anchors one commonly used way to divide the year into four distinct seasons: winter (December-February), premonsoon (March – May), monsoon (June – August), and postmonsoon (September – November). The strong and sea-

MOD08_M3.051 Aerosol Optical Depth at 550 nm [unitless]
(Jan2012 - Dec2012)

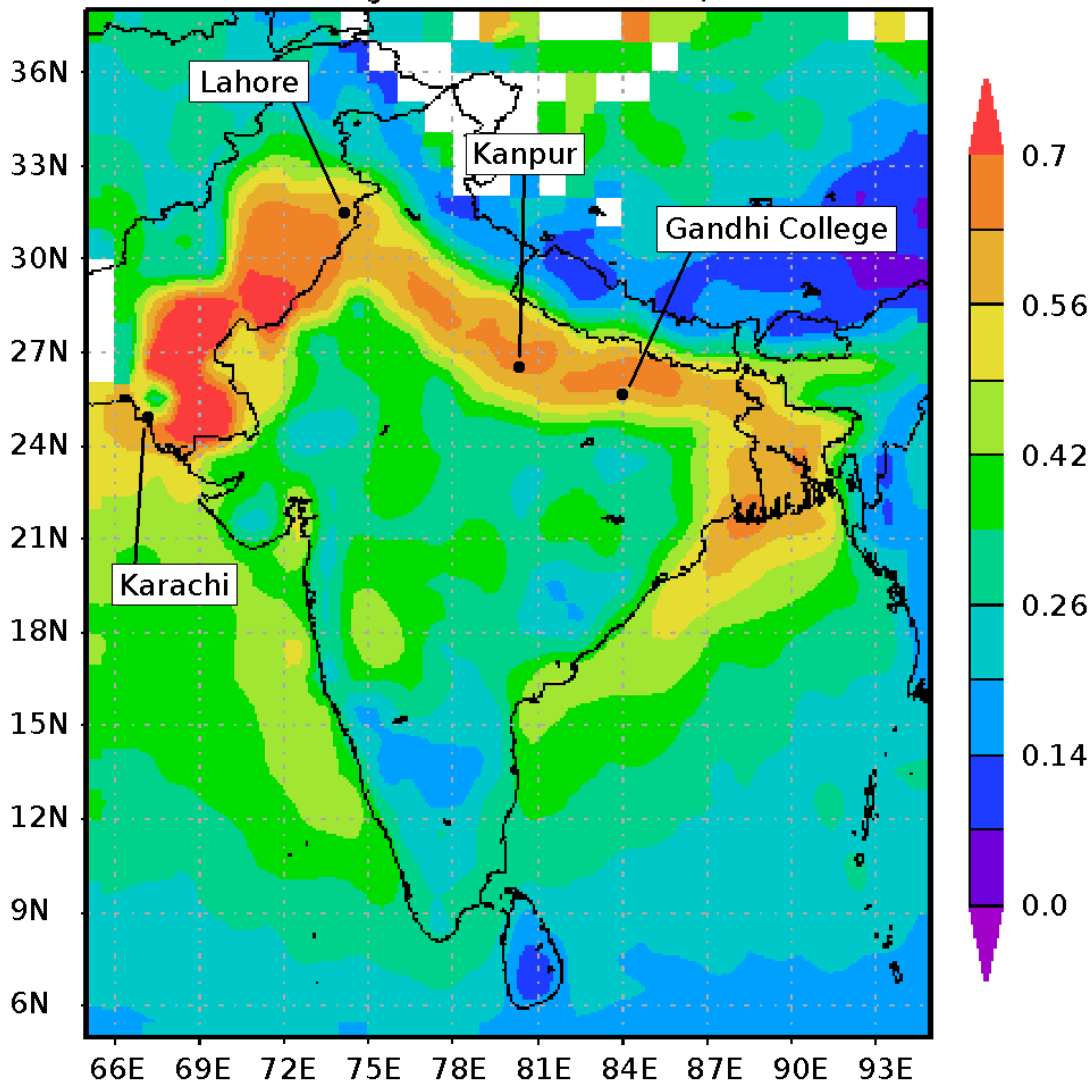


Figure 1. Annual mean AOD from MODIS Terra, with our AERONET study sites overlaid in the map. Source for MODIS data:<http://disc.sci.gsfc.nasa.gov/giovanni>.

sonally varying aerosol sources in IGP result in a very distinct geographical pattern of elevated AOD, 90 bounded in north by Himalayan foothills and to the south by lower altitude mountains.

Figure 2 shows the monthly mean AOD and SSA at 440nm for our study sites. It is noted that this data set includes all AOD values (from inversion data set) without the AOD threshold of 0.2 that we applied for refractive indices and also for SSA shown in the lower plot. This figure then further illustrates that the AOD levels are typically high and why our selected set of refractive indices was

95 not very different to “full” Level 2. The relative fractions of Level 2 data out of our selected set from Level 1.5, for refractive indices, were about 60%, 97%, 85%, and 88% for Karachi, Lahore, Kanpur, and Gandhi College, respectively.

2.2 Retrieval of BrC from AERONET measurements

Schuster et al. (2005) developed an approach to retrieve black carbon concentration and specific
100 absorption from AERONET retrievals of imaginary refractive indices and it was further extended by Arola et al. (2011) to include also BrC. Recently, this method has been further extended by Schuster et al. (2015a) to simultaneously include carbonaceous aerosols (both BC and BrC) and also mineral dust in both fine and coarse modes separately.

Since the main details of the methodology are comprehensively described elsewhere, particu-
105 larly in Schuster et al. (2015a), only main points are summarized below. The approach is based on the best match between modeled imaginary index and those retrieved by AERONET at four inversion wavelengths. For the modeled case, a scattering host is assumed to contain the following absorbing components: black carbon, brown carbon, hematite, and goethite. It is emphasized that this approach is able to detect only a subset of total organic carbon that is present, the part of ab-
110 sorbing organic carbon (BrC). Therefore, the BrC/BC ratios that we can infer from AERONET are not directly comparable with OC/BC ratios available from in-situ measurements. Table 1 provides the assumed refractive indices for each of these components. For BrC refractive index, the values given by Kirchstetter et al. (2004) were used, because globally they provide reasonable maximum and median fractions for BrC and also reasonable BrC/BC ratios. It is noted that while the most
115 recent version of Schuster et al. (2015a) uses Maxwell-Garnett as the mixing rule for refractive indices, volume averaging was assumed in the data set used in our analysis. Arguably, given the scope of our study, the choice of the mixing rule is not very essential, as long as applied consistently both in the AERONET retrieval and in our radiative transfer calculations. Moreover, it has been shown that the volume averaging results in very reasonable performance in many cases, as demonstrated
120 for instance in Lesins et al. (2002).

The AERONET-retrieved imaginary refractive indices at four wavelengths form the basis to re-
trieve the fractions of absorbing components, including BrC. The retrieval initially populates the
fine mode with BC and BrC and the coarse mode with dust components (hematite and goethite).
However, in some cases in order to reach a realistic fit with the AERONET-retrieved imaginary in-
125 dices, some of the fine mode has to additionally include iron oxides (hematite and goethite) and likewise some of the coarse mode can include carbonaceous aerosols. The average imaginary index of the three longest wavelengths (670nm, 870nm, 1020nm), at red and near-infrared and hereinafter referred to by k_{RNIR} , determines the black carbon fraction of the fine mode, for instance, while the difference between the imaginary index at 440nm and k_{RNIR} is due to the presence of BrC. Figure 3
130 shows the mean, median and variability (25% and 75% percentiles) of k_{RNIR} and of the difference

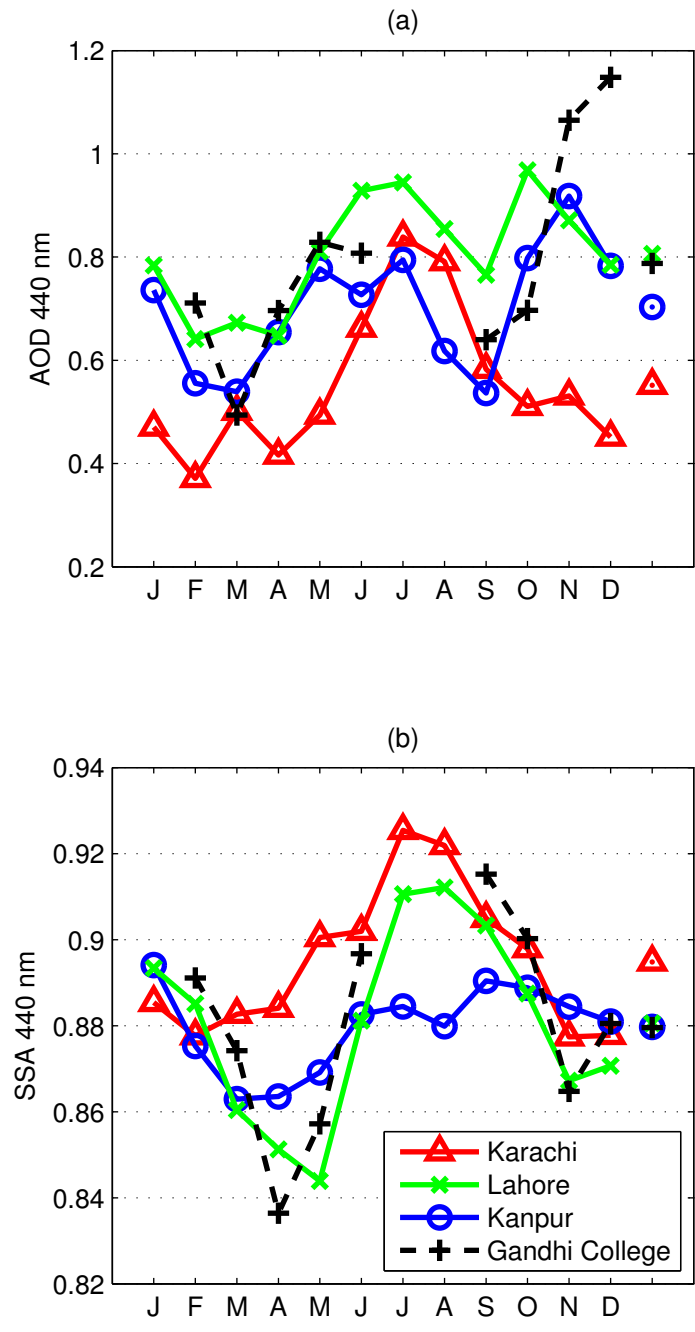


Figure 2. Monthly mean AOD and SSA at 440nm for our selected AERONET sites. Annual means are indicated by a symbol after December.

between k_{440nm} and k_{RNIR} . Very strong seasonality is evident particularly in k_{RNIR} , thus in BC. The variability is significant, nevertheless the seasonality of k_{RNIR} is strong enough that there is

no overlap between the months of highest and lowest values, between November-December and April-May, for instance. Figure 4 shows the monthly mean values of imaginary index at 440nm and the difference between k_{440nm} and k_{RNIR} , in the a) and b) panels, respectively. Table 2 gives the number of imaginary indices that was included for each site to form the monthly means. Since we use spectral imaginary index to derive BC and BrC volume fractions, there is understandably a visible similarity between BC fractions and k_{RNIR} (between panels a and c) and also BrC fractions and the difference between imaginary index at 440nm and $RNIR$ (between panels b and d). The lowest panels, in turn, show the columnar concentrations of BC and BrC. These were obtained by multiplying the BC and BrC volume fractions by AERONET-measured total volume (fine mode + coarse mode volume) and by the assumed densities. The densities of 1.8 gcm^{-3} and 1.2 gcm^{-3} were assumed for BC and BrC, respectively.

There is a significant seasonality in both components of carbonaceous aerosols, particularly in BC, largest fractions occurring in the winter and late fall seasons. This BC seasonality agrees well with the seasonal pattern that has been obtained by the surface measurements in IGP (Ram et al., 2010), who observed a very distinct BC seasonality. Moreover, they observed similar seasonal patterns for both BC and OC, highest concentrations in late fall/winter due to various sources of carbonaceous aerosols, biomass burning and wood fuel burning for domestic use, for instance. As noted before, we can only detect absorbing OC via AERONET, so our BrC pattern cannot be, therefore, directly compared with these available OC measurements. However, generally our BrC seasonality agrees also rather well with seasonality of OC in IGP observed by (Ram et al., 2010), while the clearest difference seems to be in spring, when AERONET-based BrC levels are enhanced. As shown by Vadrevu and Lasko (2015), for instance, in IGP there is a bi-modal burning season, peaking in the spring and late fall/winter; this is captured by our BrC retrievals, suggesting that a large fraction of OC emissions in spring and late fall include brown carbon.

2.3 Calculation of the radiative effect

The radiative transfer calculations were performed by using the libRadtran package (Mayer and Kylling, 2005). We used two-stream solver and correlated-k approximation of Kato et al. (1999) with bands from 1 to 31 (from 240.1 nm to 3991 nm), to cover the entire short-wave (SW) range. The direct radiative effect of BrC, DRE of BrC, at the top of the atmosphere (TOA) was calculated on a monthly basis, as the difference between two cases: including all aerosols and excluding BrC. The former was based on monthly mean size distribution and refractive index, while the latter set was formed by excluding the volume fraction of BrC. By excluding the BrC fraction, both refractive index and size distribution were then modified. The refractive index for “non-BrC” case was created by volume averaging mixing rule and including all the other components except for BrC (the scattering host, black carbon, goethite and hematite). The volume size distribution of “non-BrC” case was formed by reducing the volume in all size ranges by the volume fraction of BrC, separately in the

fine and coarse modes. By defining DRE of BrC in this fashion, aerosols are considered internally
170 mixed, which is also the case in AERONET inversion methods. We adopted similar approach to
calculate additionally DRE of BC and total aerosol.

Size distributions and refractive indices were then used for calculating the aerosol optical proper-
ties for the non-BrC mixture, which was done by utilizing the spheroid aerosol model by Dubovik
et al. (2002). The model is consistent with the one used for the retrieval of AERONET products,
175 assuming a portion of the aerosols being spheroids, as described by Dubovik et al. (2006). This
way both the “all aerosols” mixture and the “non-BrC” mixture were described by their respective
spectral AOD, SSA and asymmetry parameter, which were finally used estimating the DRE of BrC.
For the calculations of aerosol direct radiative effect, surface albedo is also a very crucial input. In
our simulations we used monthly spectral solar zenith angle dependent albedo from AERONET in-
180 version product (thus MODIS-based albedo). **The surface albedo was linearly interpolated between
the inversion data wavelengths. The surface albedo value at 440nm was extrapolated to the shorter
wavelengths as well, while the wavelengths larger than 1020nm were linearly extrapolated so that
the surface albedo at 5 μm is decreased to 0.01.** The DRE of BrC (and BC and total aerosol) at TOA
was simulated with one hour time step over a 24-hour diurnal cycle with solar insolation of the 15th
185 day of each month.

3 Results

Figure 5 shows our simulated radiative effects by BrC in the lowest panel, while the upper and middle
panels include relevant parameters to interpret these results. The difference in AOD at 440nm (in
blue) and at *RNIR* (average of 670-1020, in red) between the simulations with and without BrC is
190 shown in the upper panel. Middle panel shows similar results for SSA, which are particularly relevant
quantities now to understand whether the overall effect is warming or cooling, when BrC is added in.
It is emphasized that while brown carbon is absorbing at the shortest wavelengths, determined by the
measurement at 440nm in our case, it is almost purely scattering at *RNIR* wavelengths. Therefore,
when BrC is included, there are typically two spectrally competing effects taking place, warming at
195 the shortest and cooling at the longer wavelengths. And we can detect these effects also in the middle
panel of the Figure 5. In principle, the scattering coefficient at *RNIR* increases when BrC is added,
while the absorption coefficient remains close to a constant. Therefore, SSA (= scattering/[scattering
+ absorption]) also increases and the SSA difference at *RNIR*, shown by the dashed red lines, is
therefore essentially always positive. On the other hand, both scattering and absorption coefficients
200 increase upon addition of BrC at the 440 wavelength. Hence, SSA decreases with addition of BrC
at that wavelength, since scattering and absorption combined increases more than scattering alone.
Thus, the blue lines are always negative.

The relative strength of these spectrally separated cooling and warming effects will eventually determine whether the overall spectrally integrated shortwave direct effect is cooling or warming. And the strength of these both effects, in turn, depends on the relative fractions of other components present. In our version of absorbing components by Schuster et al. (2015a), volume averaging has been applied, consistently both in the retrieval and when we have formed new refractive indices for “non-BrC” case in our simulations. Therefore, it is also now rather straight-forward to give a quantitative estimate about the changes in the imaginary index with and without BrC at 440nm and *RNIR* range for any given fractions of these components. It is now possible to separate BrC influence this way, since we have assumed that BC has a constant refractive index at all wavelengths, where BrC is essentially non-absorbing but absorbs at 440nm. As can be seen from the Table 1, BC has the largest imaginary index at *RNIR* wavelengths and therefore the most sensitive change towards cooling at *RNIR* takes place when BrC is added to the mixture of relatively large amount of black carbon. **These changes in imaginary index, with and without BrC, essentially determine the SSA patterns we see in the middle panel of the Figure 5. Therefore, it is useful and clarifying to further interpret our BrC DRE results by focusing next on these changes.** Figure 6 shows the change in imaginary index (based on volume averaging), both at 440nm and *RNIR* range, if BrC is added in. The scale of both BC and BrC volume fractions in this figure was determined by the range retrieved for our IGP sites (in the middle panel of the Figure 4). It is evident that including BrC results in increase of imaginary index difference at 440nm, which is a strong function of BrC volume fraction but depends only slightly on the BC fraction (shown by the solid isolines of the figure). At *RNIR* range the behavior is quite different; at low enough BC fractions, BrC can result in increase in the imaginary index, however most often the opposite is true (shown by the color bar and dotted isolines of the figure). Moreover, this decrease in the imaginary index with increasing BrC volume fraction depends also relatively strongly on the BC volume fraction. This means that for a given BrC fraction, the larger the volume fraction of BC the stronger the cooling effect at *RNIR* wavelengths.

Our estimated values for DRE of BrC shown in the Figure 5, and the corresponding changes in SSA (in the middle panels), are best understood with the help of Figure 6 and there by the behavior at *RNIR* in particular. Therefore, this figure includes additionally the retrieved monthly averaged volume fractions of BC and BrC for two months, April and November, selected here to roughly represent the periods of the strongest warming and cooling. The name of the site is indicated next to the month of April, thus the other end of line corresponding to November. As can be seen from the middle panel of the Figure 5, the largest positive SSA difference at *RNIR*, when BrC is included, is in Gandhi College in November, which consistently corresponds to the case of most negative change of the *RNIR* imaginary index in the Figure 6. This is then also the case of strongest overall cooling by BrC. The spectral SSA changes due to the BrC, that are illustrated in the middle panel of the Figure 5, mainly determine whether overall cooling or warming takes place. However, the actual magnitude of these spectral cooling and warming contributions, in turn, are also substantially influ-

240 enced by the absolute BrC fractions in AOD, which are shown in the upper panel of the Figure 5. It is evident that the large values of BrC optical depths at the end of year in Gandhi College, in addition to the large increase of SSA at *RNIR* wavelengths, also strongly contribute to the considerable DRE of BrC. Brown Carbon causes cooling in the other sites as well during this time of the year, when BC fractions are at the highest. On the other hand, the warming takes place typically in the spring
245 season in all the sites, when BC fractions are lower, but BrC fractions are at relatively high levels (shown in the Figure 4 and 6). To summarize, the common pattern is the warming by BrC at spring season and cooling in the late fall and winter (except for Karachi where cooling takes place only in November-December) and this change of sign in the radiative effect by BrC is due to the different relative fractions of BC during spring and late fall seasons.

250 The annually averaged DRE of BrC is slightly positive for Karachi, while Lahore and Kanpur has slight cooling by BrC. The annually averaged negative forcing in Gandhi College is somewhat more profound due to the strongest cooling in November-December period. The strongest cooling is due to the highest total BrC concentrations and thus AOD corresponding to the BrC during this period, as can be seen from the upper panel of the Figure 5.

255 Finally, the Table 3 gives monthly DRE values for the following cases of included aerosol types: total aerosols, BrC, BC and additionally the case with all aerosols except for BrC (“non-BrC”). One can conclude, for example, that during April-May the relative magnitude of warming by BrC is about 5-7% of total aerosol cooling, except for Gandhi College, where it is as high as 20% in April due to the strong BC absorption and thus small overall cooling. On the other hand, the importance to
260 account properly for the spectral BrC effect in the DRE of carbonaceous aerosols (BrC+BC), can be emphasized by comparing it to BC (thus 2nd and 3rd rows of the Table 3). This comparison illustrates that BrC absorption can reach about 10% of carbonaceous aerosol absorption.

As discussed above, whether the spectrally integrated SW direct radiative effect by BrC results in cooling or warming is determined by the relative strength of two opposing effects, warming at
265 shorter wavelengths and cooling at *RNIR* range. Thus it is crucial to properly take both of these spectral effects into account, which is often true for total aerosol DRE calculations as well. However, it has been also common to estimate the optical properties at mid-visible only and then apply some simple approximations and assumptions to account for spectral dependence in direct radiative effect calculations (e.g., Chylek and Wong , 1995; Haywood and Shine , 1995). Therefore, we wanted to
270 also assess how well DRE based on mid-visible range only could represent the entire SW range. We repeated our calculations for DRE of BrC, but using Kato band #10 only, since it has the central wavelength at 544.8nm (range from 540 to 549.5nm). We estimated additionally direct radiative effect of BC and total aerosol, using an identical approach that we described above for BrC. Thus DRE of BC, for instance, was based on two radiative transfer runs: case of all aerosols and without
275 BC. We then calculated the mean ratio of DRE from the following two runs (separately for BrC, BC and total aerosol cases): 1) actual spectrally resolved radiative transfer calculation including all

the Kato bands, i.e. by the same approach we have applied in our results shown earlier, 2) radiative effect from a single Kato band #10 only. This mean ratio was then used as a conversion factor to get a full SW DRE from a single-band DRE radiative transfer runs, and to make these two approaches comparable. Figure 7 shows the DRE in Kanpur from these two cases: 1) actual spectrally resolved radiative transfer calculation including all the Kato bands, 2) radiative effect from a single Kato band #10 only, but scaled to represent full SW.

It is evident that a single wavelength approach can produce a rather stable estimate for BC radiative effect, the relative error is within $\pm 10\%$, which is understandable given spectrally invariant imaginary index of BC. On the other hand, both BrC and total aerosol cases can reach significantly higher relative differences. SW radiative effects of BrC and total aerosol include typically wavelength ranges of both cooling and warming effects that a single wavelength approach cannot therefore properly capture. Spectral dependence of DRE of BrC was illuminated above, while the spectral dependence of total aerosol DRE is typically different; for instance in Kanpur SSA is low enough and surface albedo high enough at *RNIR* range during summer months to produce warming at these longer wavelengths (not shown), although the overall spectrally integrated total aerosol direct radiative effect is always negative, as shown in the lower panel of the Figure 7

4 Conclusions

The importance of light absorbing organic aerosols has become evident in recent years. It is important to understand and take into account the effects of BrC not only for the aerosol radiative forcing, but also for surface UV radiation levels and remote sensing from satellite in the UV wavelengths. However, there are relatively few measurement-based estimates for the direct radiative effect of BrC so far. In those earlier studies, the AERONET-measured AAOD and AAE have been exploited, while this is the first time that DRE of BrC is estimated by exploiting the AERONET-retrieved imaginary indices. **With AAOD and AAE information only, there is little information about the aerosol size and thus the separation of dust and BrC absorption becomes unclear, while arguably with the use of imaginary indices (Schuster et al., 2015b) they can be better distinguished.** We estimated the radiative effect of BrC for four AERONET sites in Indo-Gangetic Plain (IGP), Karachi, Lahore, Kanpur and Gandhi College. We found a distinct seasonality, which was generally similar among all the sites, but with slightly different strengths. The warming by BrC takes place during spring season, due to the relatively low BC fractions so that the scattering effect by BrC at *RNIR* does not become significant enough and the absorption at the shortest wavelengths is dominating in the spectrally integrated radiative effect. Opposite is true in late fall and in the winter period, when the BC fractions are more substantial and therefore the cooling effect at *RNIR* wavelengths becomes more significant in the overall shortwave radiative effect by BrC.

We estimated the DRE of BrC as a difference of two radiative transfer runs: case of all aerosols and without BrC. We estimated the DRE of BC and total aerosol similarly and in that context, it became evident that the role of BrC is not insignificant and, moreover, it is crucial to properly account for its spectral radiative effect. The DRE of BrC can reach magnitudes of 10% relative to BC, so it is not negligible in the DRE of absorbing carbonaceous (BC+BrC) aerosols. Moreover, DRE of BrC exhibited a distinct seasonality in the four sites we included in our analysis. Therefore, this study stresses the need to account for absorbing OC, not to assume it purely scattering. And it is then particularly crucial to properly account for both warming at the lowest and cooling effect at the longer wavelengths, when forming the overall SW direct radiative effect of BrC.

320 *Acknowledgements.* This study was supported by the Academy of Finland (project number 264242).

References

- Arola, A., Schuster, G., Myhre, G., Kazadzis, S., Dey, S., and Tripathi, S. N.: Inferring absorbing organic carbon content from AERONET data, *Atmospheric Chemistry and Physics*, 11, 215–225, <http://www.atmos-chem-phys.net/11/215/2011/>, 2011.
- 325 Chung, C., Ramanathan, V., and Decremer, D.: Observationally constrained estimates of carbonaceous aerosol radiative forcing, *Proc. Natl. Acad. Sci.*, 109, 11 624–11 629, 2012.
- Chylek, P. and J., Wong, J., Effect of absorbing aerosols on global radiation budget. *Geophys. Res. Lett.*, 22, 929–931, 1995.
- Dubovik, O., A. Smirnov, B. N. Holben, M. D. King, Y. J. Kaufman, T. F. Eck, and I. Slutsker, Accuracy
330 assessment of aerosol optical properties retrieval from AERONET sun and sky radiance measurements, *J. Geophys. Res.*, 105, 9791–9806, 2000.
- Dubovik, O. and Holben, B. N. and Lapyonok, T. and Sinyuk, A. and Mishchenko, M. I. and Yang, P. and Slutsker, I.: Non-spherical aerosol retrieval method employing light scattering by spheroids, *Geophysical Research Letters*, 29, 54–1–54–4, doi:10.1029/2001GL014506, 2002.
- 335 Dubovik, Oleg and Sinyuk, Alexander and Lapyonok, Tatyana and Holben, Brent N. and Mishchenko, Michael and Yang, Ping and Eck, Tom F. and Volten, Hester and Muñoz, Olga and Veihelmann, Ben and van der Zande, Wim J. and Leon, Jean-Francois and Sorokin, Michael and Slutsker, Ilya, Application of spheroid models to account for aerosol particle nonsphericity in remote sensing of desert dust, *Journal of Geophysical Research: Atmospheres*, 111, doi:10.1029/2005JD006619, 2006.
- 340 Eck, T., Holben, B., Reid, J. S., Dubovik, O., Smirnov, A., O'Neill, N. T., Slutsker, I., and Kinne, S., Wavelength dependence of the optical depth of biomass burning urban and desert dust aerosols, *J. Geophys. Res.*, 104, 31333–31349, doi:10.1029/1999JD900923, 1999.
- Feng, Y., Ramanathan, V., and Kotamarthi, V. R.: Brown carbon: a significant atmospheric absorber of solar radiation?, *Atmos. Chem. Phys.*, 13, 8607–8621, doi:10.5194/acp-13-8607-2013, 2013.
- 345 Haywood, J. M. and K. P., Shine, K. P., The effect of anthropogenic sulfate and soot aerosol on the clear sky planetary radiation budget. *Geophys. Res. Lett.*, 22, 602–606, 1995.
- Holben B.N., T.F. Eck, I. Slutsker, D. Tanre, J.P. Buis, A. Setzer, E. Vermote, J.A. Reagan, Y. Kaufman, T. Nakajima, F. Lavenu, I. Jankowiak, and A. Smirnov, AERONET - A federated instrument network and data archive for aerosol characterization, *Rem. Sens. Environ.*, 66, 1-16, 1998.
- 350 Jethva, H., S. K. Satheesh, and J. Srinivasan, Seasonal variability of aerosols over the Indo-Gangetic basin, *J. Geophys. Res.*, 110, D21204, doi:10.1029/2005JD005938, 2005.
- Kanakidou, M., Seinfeld, J. H., Pandis, S. N., Barnes, I., Dentener, F. J., Facchini, M. C., Van Dingenen, R., Ervens, B., Nenes, A., Nielsen, C. J., Swietlicki, E., Putaud, J. P., Balkanski, Y., Fuzzi, S., Horth, J., Moortgat, G. K., Winterhalter, R., Myhre, C. E. L., Tsigaridis, K., Vignati, E., Stephanou, E. G., and Wilson, J.: Organic
355 aerosol and global climate modelling: a review, *Atmos. Chem. Phys.*, 5, 1053–1123, 2005.
- Kato, S., Ackerman, T., Mather, J., and Clothiaux, E.: The k-distribution method and correlated-k approximation for short-wave radiative transfer model, *J. Quant. Spectrosc. Ra.*, 62, 109–121, 1999.
- Kedia, S., S. Ramachandran, B.N. Holben, and S.N. Tripathi, Quantification of aerosol type, and sources of aerosols over the Indo-Gangetic Plain, *Atmospheric Environment*, Volume 98, p. 607-619,
360 <http://dx.doi.org/10.1016/j.atmosenv.2014.09.022>, 2014.

- Kirchstetter, T. W., T. Novakov, and P. V. Hobbs, Evidence that the spectral dependence of light absorption by aerosols is affected by organic carbon, *J. Geophys. Res.*, 109, D21208, doi:10.1029/2004JD004999, 2004.
- Lesins, G., P. Chylek, and U. Lohmann, A study of internal and external mixing scenarios and its effect on aerosol optical properties and direct radiative forcing, *J. Geophys. Res.*, 107(D10),
365 doi:10.1029/2001JD000973, 2002.
- Lu, Z., Streets, D. G., Winijkul, E., Yan, F., Chen, Y., Bond, T. C., Feng, Y., Dubey, M. K., Liu, S., Pinto, J. P. and Carmichael, G. R., Light Absorption Properties and Radiative Effects of Primary Organic Aerosol Emissions, *Environmental Science & Technology*, 49, 8, 4868-4877, 10.1021/acs.est.5b00211, 2015.
- Martins, J. V., P. Artaxo, Y. J. Kaufman, A. D. Castanho, and L. A. Remer, Spectral absorption properties of
370 aerosol particles from 350-2500nm, *Geophys. Res. Lett.*, 36, L13810, doi:10.1029/2009GL037435, 2009.
- Mayer, B. and Kylling, A.: Technical note: The libRadtran software package for radiative transfer calculations - description and examples of use, *Atmos. Chem. Phys.*, 5, 1855-1877, doi:10.5194/acp-5-1855-2005, 2005.
- Myhre, G., D. Shindell, F.-M. Bréon, W. Collins, J. Fuglestedt, J. Huang, D. Koch, J.-F. Lamarque, D. Lee, B. Mendoza, T. Nakajima, A. Robock, G. Stephens, T. Takemura and H. Zhang, Anthropogenic and Natural
375 Radiative Forcing. In: *Climate Change 2013: The Physical Science Basis. Contribution of Working Group I to the Fifth Assessment Report of the Intergovernmental Panel on Climate Change* [Stocker, T.F., D. Qin, G.-K. Plattner, M. Tignor, S.K. Allen, J. Boschung, A. Nauels, Y. Xia, V. Bex and P.M. Midgley (eds.)]. Cambridge University Press, Cambridge, United Kingdom and New York, NY, USA, 2013.
- Ram, K., M. M. Sarin, and S. N. Tripathi, A 1 year record of carbonaceous aerosols from an urban site in
380 the Indo-Gangetic Plain: Characterization, sources, and temporal variability, *J. Geophys. Res.*, 115, D24313, doi:10.1029/2010JD014188, 2010.
- Schuster, G. L., O. Dubovik, B. N. Holben, and E. E. Clothiaux, Inferring black carbon content and specific absorption from Aerosol Robotic Network (AERONET) aerosol retrievals, *J. Geophys. Res.*, 110, D10S17, doi:10.1029/2004JD004548, 2005.
- 385 Schuster, G. L., Dubovik, O., and Arola, A.: Remote sensing of soot carbon – Part 1: Distinguishing different absorbing aerosol species, *Atmos. Chem. Phys. Discuss.*, 15, 13607-13656, doi:10.5194/acpd-15-13607-2015, 2015a.
- Schuster, G. L., Dubovik, O., Arola, A., Eck, T. F., and Holben, B. N.: Remote sensing of soot carbon – Part 2: Understanding the absorption Angstrom exponent, *Atmos. Chem. Phys. Discuss.*, 15, 20911-20956,
390 doi:10.5194/acpd-15-20911-2015, 2015b.
- Schuster G., O. Dubovik, and A. Arola, Remote sensing of soot carbon, Part 2: Understanding the absorption Angstrom exponent, submitted to *Atmos. Chem. Phys.*, 2015b.
- Vadrevu, K. and K. Lasko, Fire regimes and potential bioenergy loss from agricultural lands in the Indo-Gangetic Plains, *Journal of Environmental Management*, Volume 148, p. 10-20,
395 <http://dx.doi.org/10.1016/j.jenvman.2013.12.026>, 2015.
- Zhang, Q., Jimenez, J. L., Canagaratna, M. R., Allan, J. D., Coe, H., Ulbrich, I., Alfarra, M. R., Takami, A., Middlebrook, A. M., Sun, Y. L., Dzepina, K., Dunlea, E., Docherty, K., DeCarlo, P. F., Salcedo, D., Onasch, T., Jayne, J. T., Miyoshi, T., Shimojo, A., Hatakeyama, S., Takegawa, N., Kondo, Y., Schneider, J., Drewnick, F., Borrmann, S., Weimer, S., Demerjian, K., Williams, P., Bower, K., Bahreini, R., Cottrell, L., Griffin, R. J.,
400 Rautiainen, J., Sun, J. Y., Zhang, Y. M., and Worsnop, D. R., Ubiquity and dominance of oxygenated species

in organic aerosols in anthropogenically-influenced Northern Hemisphere midlatitudes, *Geophys. Res. Lett.*,
34, L13801, doi:10.1029/2007GL029979, 2007.

Table 1. Imaginary indices at 440nm and NIR (average of 670,870, and 1020nm) assumed for each component in the retrieval of Schuster et al. (2015a).

Wavelength	BrC	BC	Goethite	Hematite
440	0.063	0.79	0.068	1.23
NIR	0.003	0.79	0.1203	0.127

Table 2. Number of AERONET observations for each month for the four sites. Data was collected for Karachi from 9/2006 to 8/2011, for Lahore from 4/2007 to 10/2011, for Kanpur from 1/2001 to 4/2012 and for Gandhi College from 4/2006 to 3/2010. Monthly data in parenthesis was not included in the study due to low number of observations.

Month	Karachi	Lahore	Kanpur	Gandhi College
1	121	19	389	(7)
2	105	13	543	23
3	176	107	746	149
4	165	186	535	211
5	136	172	626	307
6	90	139	365	109
7	46	83	49	(8)
8	14	45	62	(5)
9	129	96	253	42
10	239	116	508	72
11	173	114	433	54
12	118	10	466	68

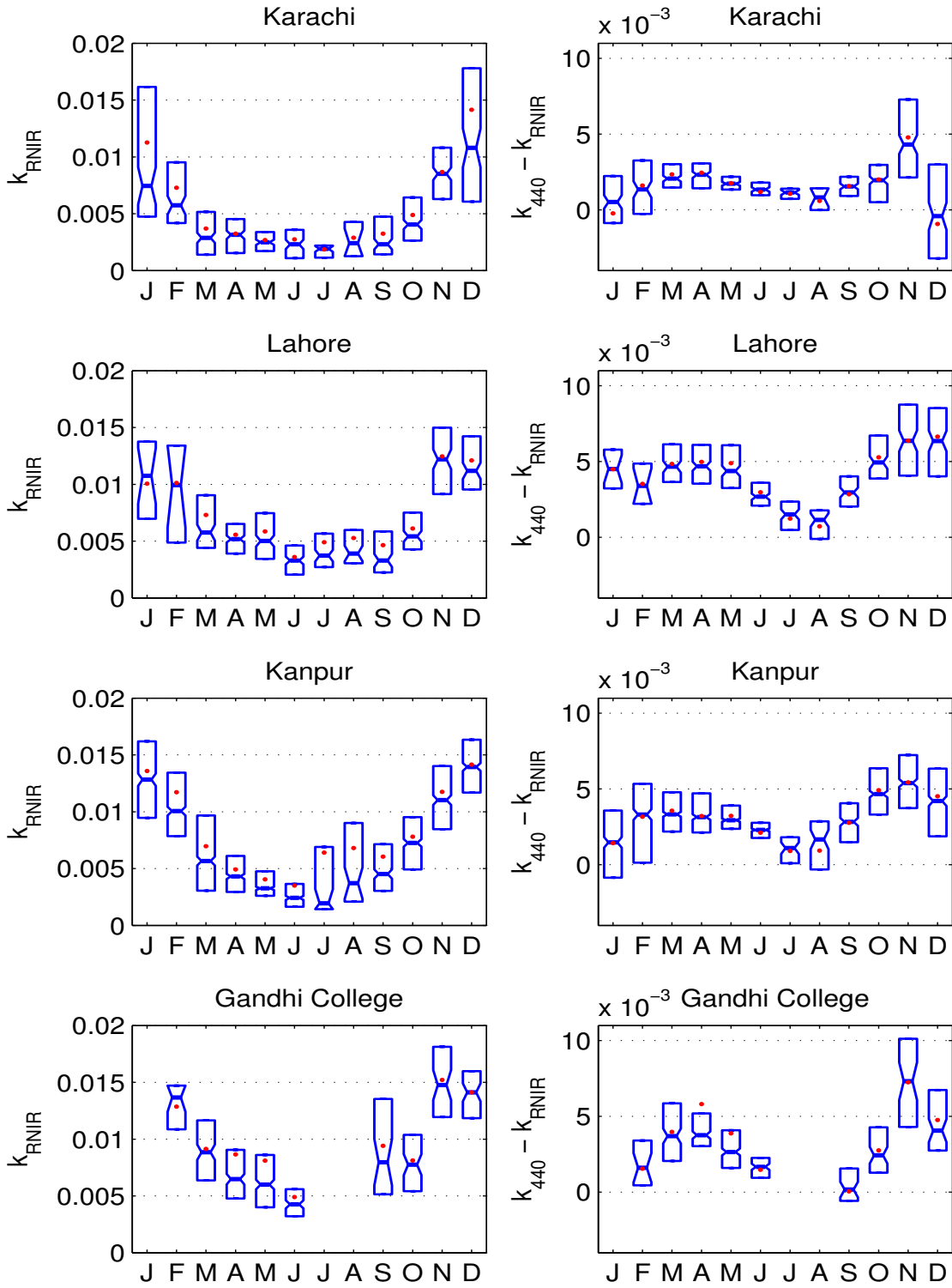


Figure 3. Boxplot of monthly imaginary indices: average of imaginary index at 670nm, 870nm, and 1020nm (k_{RNIR}) in the left panel; difference between the imaginary index at 440nm and k_{RNIR} in the right panel, showing 25% and 75% percentiles. Box-plot indicates the median and mean is additionally shown by red dots.

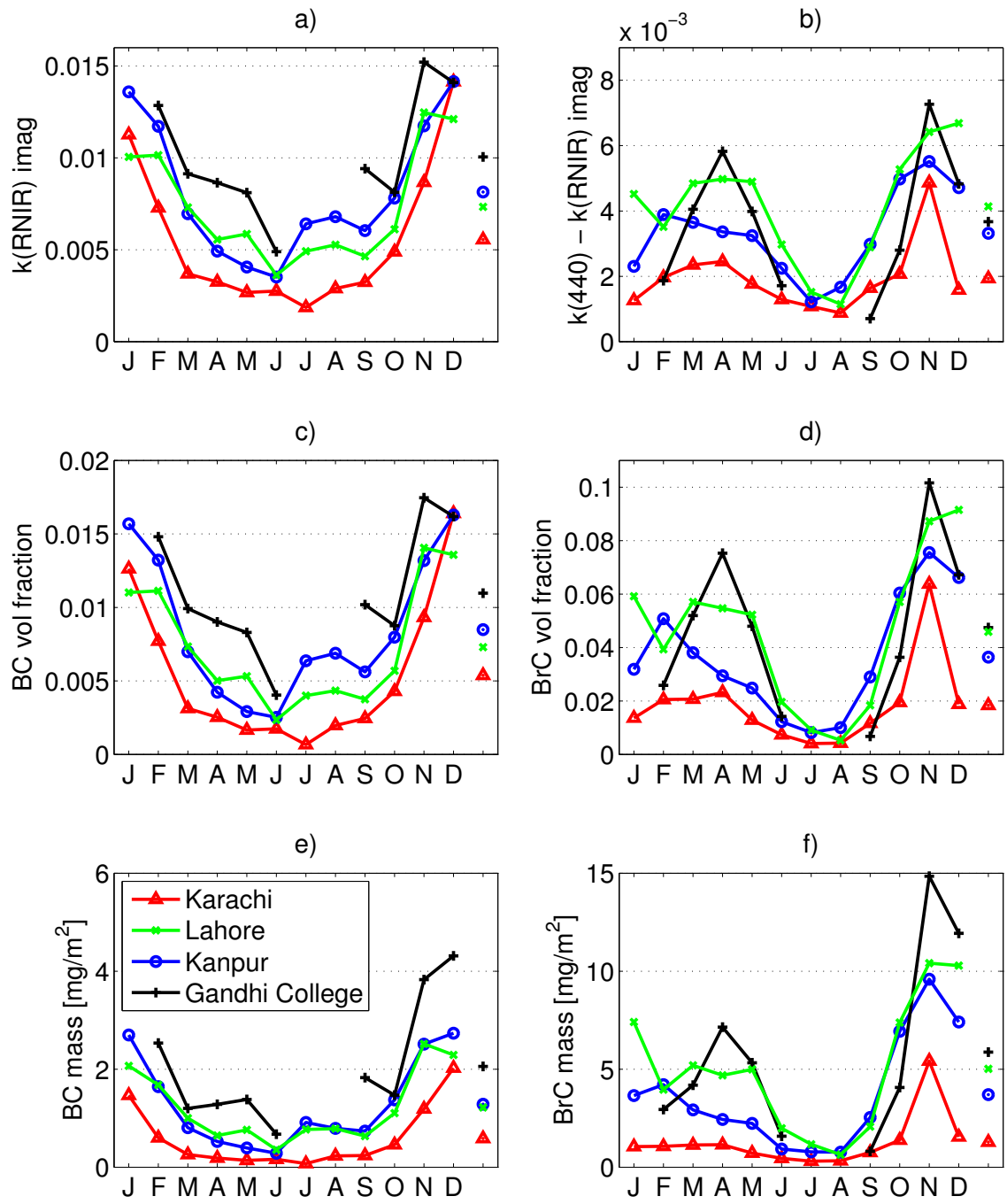


Figure 4. Monthly averages of imaginary indices and the retrieved fraction of carbonaceous aerosols: a) average of imaginary index at 670nm, 870nm, and 1020nm (k_{RNIR}); b) difference between the imaginary index at 440nm and k_{RNIR} ; retrieved volume fractions of c) BC and d) BrC; retrieved columnar concentrations in [mg/m^2] of e) BC and f) BrC. Corresponding annual averages are given after December.

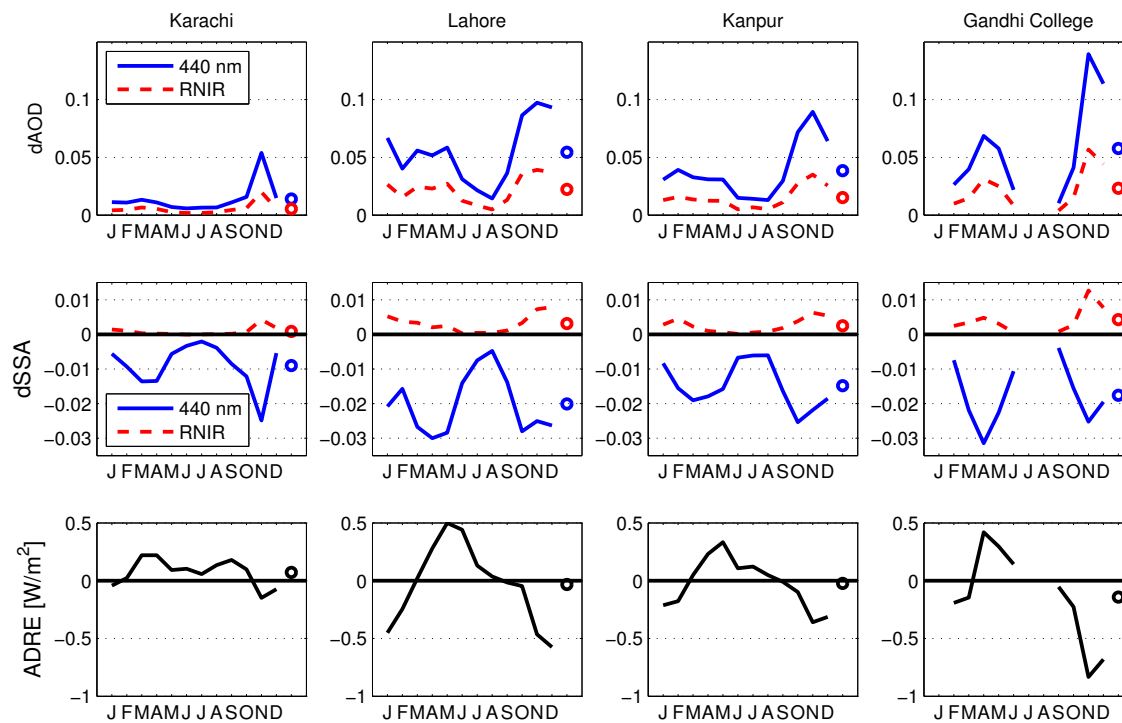


Figure 5. Upper panel: monthly averages of difference in AOD at 440nm (blue) and at *RNIR* (red) between simulations with and without BrC. Middle panel: corresponding cases for SSA. Lower panel: monthly average DRE of BrC. Corresponding annual averages are given by the symbol after December.

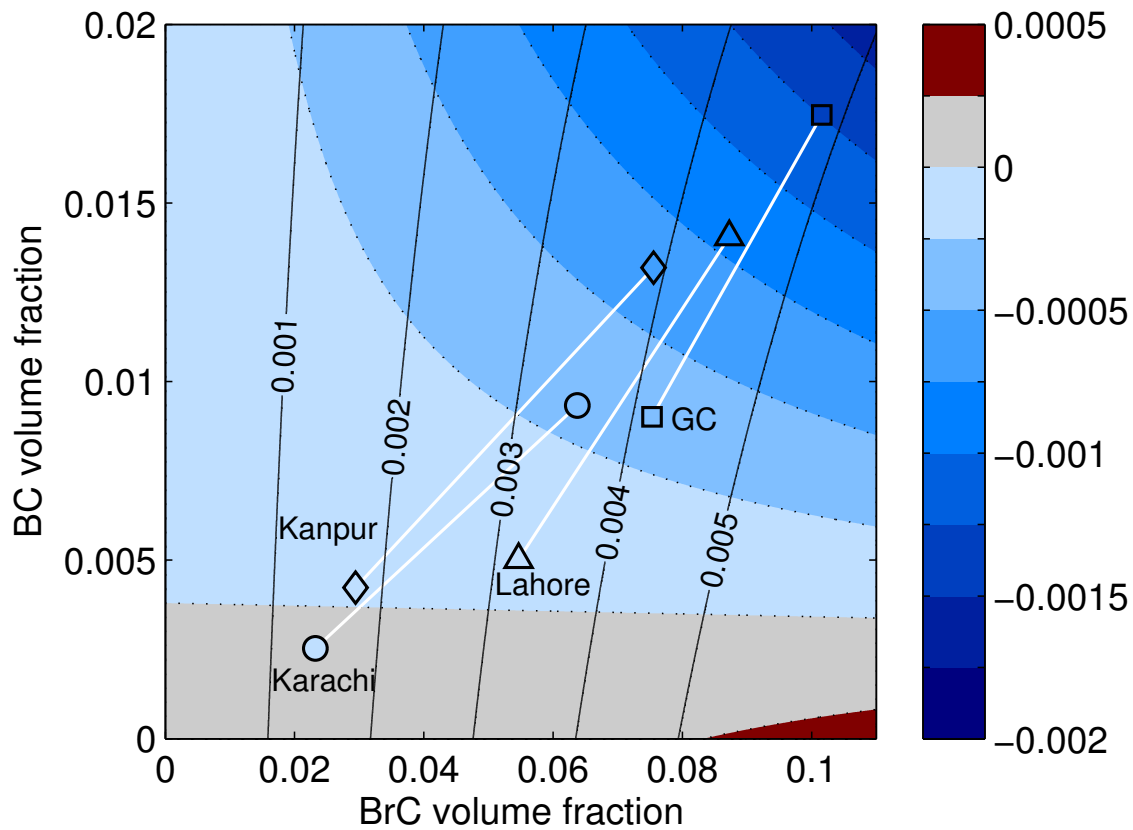


Figure 6. Difference between imaginary index with and without BrC included at 440nm (solid isolines) and at *RNIR* wavelengths (by color bar and dotted isolines) as a function of BC and BrC volume fractions. Monthly mean values of BC and BrC volume fractions are shown for each site by symbols and lines for two months: April with the name of the site next to it and November in the other end of the line.

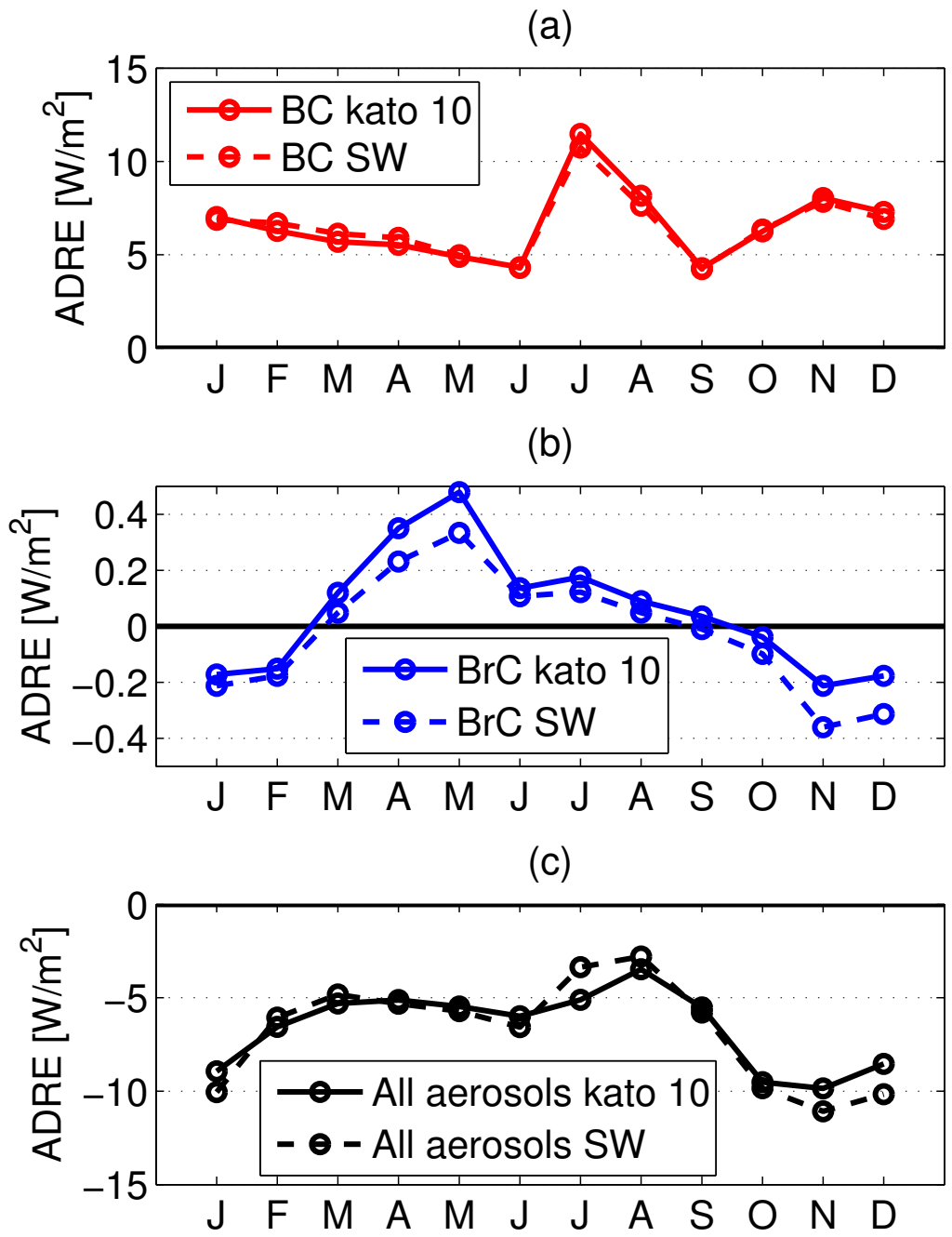


Figure 7. Direct radiative effect in Kanpur based on two spectral ranges of Kato bands: 1) All Kato bands and 2) Kato band #10 (center wavelength at 544.8nm), but scaled to account for full SW range. Upper panel: for BC; Middle panel: for BrC; lower panel: for total aerosol.

Table 3. Monthly DRE [W/m^2] of different aerosol types, “non-BrC” referring to case with all the other aerosols than BrC. Annual mean is shown after December. Three missing months of Gandhi College had less than 10 observations.

	Jan	Feb	Mar	Apr	May	Jun	Jul	Aug	Sep	Oct	Nov	Dec	Annual
Karachi													
Total	-6.06	-4.72	-6.30	-4.72	-5.67	-6.18	-11.28	-7.55	-5.91	-7.08	-6.81	-5.62	-6.49
BrC	-0.04	0.02	0.22	0.22	0.09	0.10	0.06	0.13	0.18	0.10	-0.15	-0.07	0.07
BC	5.91	4.66	3.54	2.25	1.42	2.73	0.93	3.92	3.22	3.57	4.99	6.06	3.60
non-BrC	-6.02	-4.75	-6.52	-4.94	-5.76	-6.28	-11.34	-7.69	-6.09	-7.18	-6.66	-5.55	-6.56
Lahore													
Total	-12.82	-10.27	-7.98	-7.18	-6.62	-9.42	-10.29	-8.95	-10.23	-13.72	-11.48	-10.92	-9.99
BrC	-0.45	-0.24	0.02	0.28	0.50	0.44	0.13	0.04	-0.02	-0.05	-0.46	-0.57	-0.03
BC	5.00	5.75	6.61	5.92	8.35	4.83	6.96	6.29	4.30	5.90	7.51	5.70	6.09
non-BrC	-12.37	-10.03	-8.01	-7.46	-7.12	-9.86	-10.42	-8.99	-10.22	-13.67	-11.01	-10.34	-9.96
Kanpur													
Total	-10.05	-6.06	-4.83	-5.32	-5.72	-6.57	-3.36	-2.79	-5.80	-9.84	-11.08	-10.16	-6.80
BrC	-0.21	-0.18	0.05	0.23	0.33	0.11	0.12	0.05	-0.01	-0.10	-0.36	-0.31	-0.02
BC	6.88	6.71	6.13	5.91	4.98	4.30	10.74	7.63	4.24	6.35	7.84	6.93	6.55
non-BrC	-9.84	-5.88	-4.88	-5.55	-6.06	-6.67	-3.48	-2.84	-5.79	-9.74	-10.72	-9.85	-6.78
Gandhi College													
Total	-	-9.18	-6.51	-2.08	-3.88	-9.06	-	-	-7.31	-10.14	-10.42	-13.00	-7.95
BrC	-	-0.19	-0.15	0.42	0.30	0.14	-	-	-0.05	-0.23	-0.83	-0.68	-0.14
BC	-	7.56	5.36	9.92	10.83	6.44	-	-	5.42	5.51	9.53	8.73	7.70
non-BrC	-	-8.98	-6.36	-2.50	-4.18	-9.20	-	-	-7.26	-9.92	-9.59	-12.32	-7.81